Electronic Supplementary Material (ESI) for Energy & Environmental Science.
This journal is © The Royal Society of Chemistry 2020

Supplementary Information

High carbonate ion conductance of robust PiperION membrane allows industrial current density and conversion in zero-gap carbon dioxide electrolyzer cell

B. Endrődi,[a,*] E. Kecsenovity,[a] A. Samu,[a] T. Halmágyi,[a] S. Rojas-Carbonell,[b] L. Wang,[b] Y. Yan[b], C. Janáky[a,c,*]

[a]Department of Physical Chemistry and Materials Science, Interdisciplinary Excellence Centre, University of Szeged, Aradi Square 1, Szeged, H-6720, Hungary

[b]W7energy LLC, 200 Powder Mill Rd, E500-2440, Wilmington, DE, 19803, United States of America

[c]ThalesNanoEnergy Zrt, Alsó Kikötő sor 11, Szeged 6726, Hungary

Experimental Section

Materials used

All chemicals were purchased from commercial suppliers (Sigma-Aldrich and VWR International), and were of at least analytical grade and were used without further purification. MilliQ grade (ρ = 18.2 MΩ cm) ultrapure deionized water was used to prepare all the solutions.

Measurement of through plane membrane conductivity

The Scribner 740 Membrane Test System equipped with the Newtons4th PSM1735 + IAI frequency response analyzer were used to measure the through plane conductivity of the membranes. Membranes were cut to dimensions of 10 mm by 30 mm and exchanged to the desired anion by immersing three times in 50 cm^3 of 0.5 M sodium bicarbonate or carbonate solution for an hour each time. After the ion exchange, the membranes were washed with running DI water for 5 minutes.

The platinum electrodes of the through plane cell head were coated with conductive carbon paint (SPI Supplies, colloidal graphite, Part #05006-AB) and gas diffusion layers (E-TEK, High Temperature ELAT, 140E–W). The exchanged membrane was placed in between the two electrodes with a 10% compression and the cell introduced in the chamber of the membrane testing system.

The testing protocol consisted a presoaking period of 2 hours, where the membrane sample was exposed to the target temperature and a 95% relative humidity to allow for the full hydration and equilibration of the membrane prior to the measurement. After the presoaking period, the membrane impedance was measured between 1 Hz and 20 MHz with a 10 mV AC signal.

Electrode preparation and membrane pretreatment

A 25 mg cm^{-3} dispersion of Ag nanoparticles (d_{avg} < 100 nm, Sigma-Aldrich) containing 15 wt% of the ionomer supplied with the used AEM was prepared, using a 1:1 isopropanol-water solvent mixture. Similarly, a 20 mg cm^{-3} dispersion of Ir nanoparticles (Fuel-Cell Store) were formed in an identical solvent mixture and ionomer concentration. The Ir dispersion was homogenized in a regular ultrasonic bath for 20 minutes (keeping the bath temperature below 35 °C), while a high-power immersion sonotrode was used to disperse the silver nanoparticles.

A hand-held airbrush and compressed air carrier gas (~100 cm^3 min^{-1}) was used to immobilize the silver dispersion on the microporous layers of preheated (100 °C) Sigracet 39BC carbon gas diffusion layers. The anode catalyst was spray-coated similarly, on a porous Ti-frit. The anode and cathode catalyst loadings were both 1.0 ± 0.1 mg cm^{-2}.

The membranes were activated overnight by immersing them in 1 M CsOH (or KOH). Subsequently it was cut into shape using a surgical blade, washed with ample amount of DI water, and inserted in the electrolyzer cell in its fully hydrated form. Four commercially available membranes were used in this study: Selemion AMV (AGC), Fumasep-FAB-PK-130 (Fumatech GmbH), bare and PTFE-supported Sustainion® X37-50 (Dioxide Materials) and PiperION TP-85 (W7energy) having different thickness (15, 32, 50, and 80 μm).

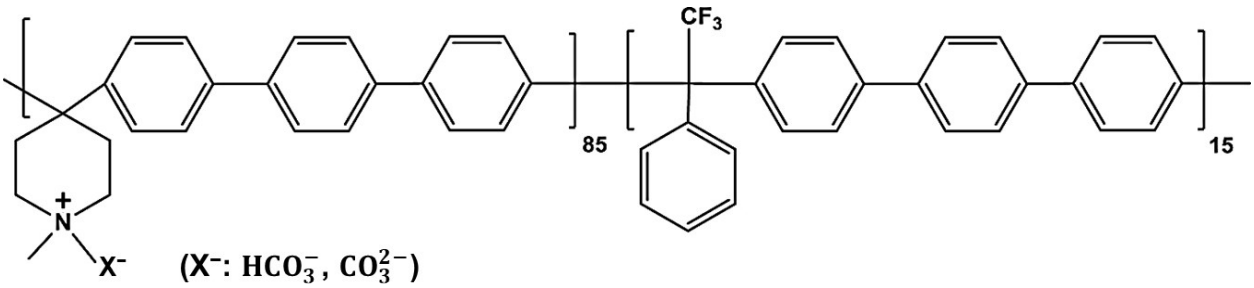

Fig. S1. Chemical structure of the PiperION TP-85 membrane.

Cell assembly

Similarly to our previous study (ref. #23 in the main text), a custom-designed direct gas feed, zero-gap cell was used for the measurements (8 cm^2 active area). In this study, a membrane was mounted between a cathode GDE and a 2 mm thick Ti frit anode, with the catalyst layers facing the membrane. Two PTFE or PEEK rings were used to hold the electrodes in position, and to control the compression of the GDE. Flow-channels were formed in the current collectors, directly pressing the electrodes together. Importantly, a CO_2 gas inlet was formed in the center of the circular cathode current collector, while the outlet channel is on the perimeter. 6 bolt screws were used to assemble the cell, gradually applying a torque of 3 Nm. The gas tightness of the electrolyzer was ensured by EPDM rubber (Ethylene propylene diene monomer) O-rings between the cell components. Similar gas-flow channels and sealing concept was utilized in the 100 cm^2-sized cell (co-developed by the University of Szeged and ThalesNanoEnergy Zrt), except its rectangular shape.

Cell testing

The electrolyzer cell was tested in a slightly upgraded version of the test environment demonstrated in our previous study (ref. #23 in the main text). Shortly, the CO_2 gas flow-rate was controlled by Bronkhorst mass-flow controller. The gas was passed through a heated humidifier before entering the cell. The anolyte was heated on a water bath and circulated in the anode compartment by a peristaltic pump. The humid product gas stream leaving the cathode was passed through a two-step mechanical and thermal water separation before entering the gas chromatograph. The pressure of the CO_2 gas was controlled by a Swagelok spring-loaded back-pressure regulator, and read from precision, analogue pressure gauges. The temperature of the anode and cathode compartments were monitored by digital thermometers, placed directly in small holes drilled in the current collector in the close vicinity of the membrane. The gas flow-rate was measured using an Agilent digital ADM flow meter, and a classical soap bubble flow-meter.

Electrochemical measurements

Electrochemical measurements were performed using a Biologic VMP-300 type potentiostat/galvanostat in a 2-electrode setup. Electrochemical impedance spectra were recorded between 1 Hz-100 kHz with 10 mV RMS perturbation. The consistency of the EIS data was confirmed by performing the Kramers–Kronig test.

Product analysis

The product stream composition was analyzed using a Shimadzu GC-2010 Plus instrument, equipped with a barrier discharge ionization (BID) detector, a Restek ShinCarbon ST column and 6.0 grade Helium carrier gas. An automatized 6-port valve was used to take samples at regular time intervals. A calibration was performed prior the experiments using pure gases and calibration gas mixtures containing H_2, CO and CO_2 in different volumetric ratios between 0.5 − 50 %. The anode gas was analyzed with a BGA-244 type Binary Gas Analyzer (Stanford Research Systems), to monitor the CO_2/O_2 ratio.

X-ray micro-computed tomography (micro-CT) analysis

A BrukerSkyScan 2211 instrument using a tungsten target, operating with a source voltage of 50 kV and a current of 600 µA was used to record micro-CT images of the compressed GDEs. The open filter assembly was used to allow the sample stage to be in the closest proximity of the X-ray source. The images were re-constructed with the help of the commercially available NRecon Reconstruction Software and the CtVox software (Skyscan, Bruker, Belgium).

The important metrics, which together describe the cell operation are:

- Faradaic efficiency: the fraction of the total charge used in the electrochemical reaction of interest (i.e., carbon monoxide formation) at given cell voltage/current,
- Single-pass conversion: the portion of the CO_2 reactant converted into *any* reduction product when passing through the electrochemical cell,
- Full cell energy efficiency: the relative cell voltage required to drive the process at a given current density compared to thermodynamic cell voltage (e.g., $\Delta U_{thermodynamic,\ CO} = 1.33\ V / \Delta U_{cell} \times 100\ \%$).

Structure of the GDE mounted in the electrolyzer cell

A custom-designed direct gas feed, zero-gap cell was employed in all our experiments, which allowed changing and hence tailoring the level of GDE compression to effectively force the gas in the porous substrate, and to the catalyst layers. We found in our exploratory measurements that compressing the cathode GDL by about 15 % results in the best electrochemical performance of the electrolyzer cell. This ensures proper electronic coupling between the components without damaging the carbon paper structure, while also forces the CO_2 gas in the pore system (Fig. S2A). We note that the optimal degree of compression depends on the width of the gas channels and gas pattern as well, therefore it is to be optimized when a new electrolyzer design is applied.

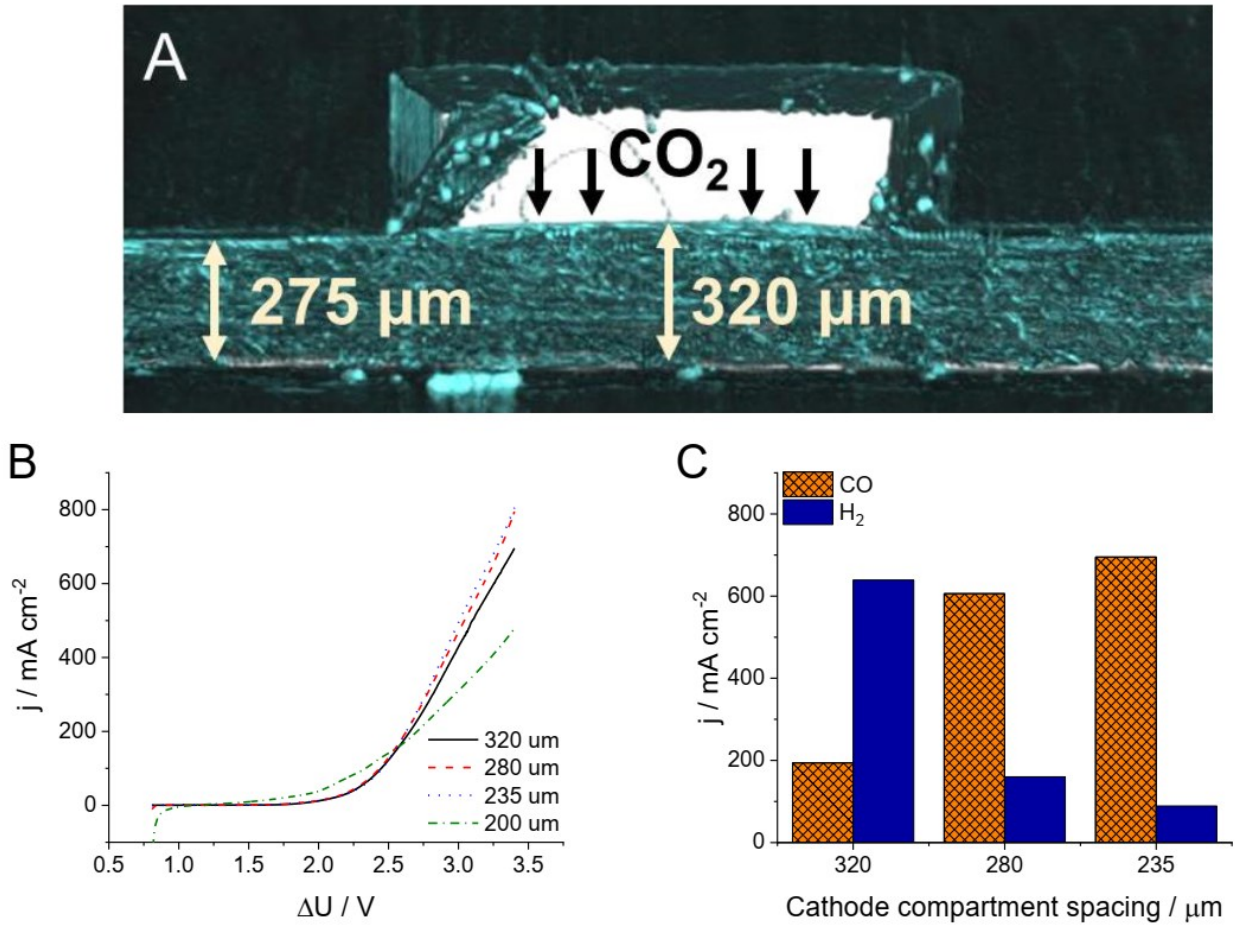

Fig. S2. (A) MicroCT image on the slight compression of the GDE, showing how the gas is forced into the carbon paper. (B) LSV curves and (C) partial current densities for CO and H_2 formation during chronoamperometric measurements at $\Delta U = 3.4$ V, recorded for an electrolyzer cell with 32 µm thick PiperION membrane, at different cathode compartment spacings. The measurements in (B) and (C) were performed applying 0.1 M CsOH anolyte at $T_{cell} = 60$ °C, with 12.5 cm^3 min^{-1} cm^{-2} CO_2 feed rate.

The compression level of the GDE determines the electrochemical properties of the cell as shown by our LSV (Fig. S2B) and chronoamperometric measurements (Fig. S2C). Similar total current densities were observed on the LSV curves with the non-compressed (320 μm), ~15 % (280 μm) and ~30 % (235 μm) compressed GDEs. Further compression (~40 %, 200 μm) resulted in a current decrease and rapid cell failure during subsequent measurements. This is probably caused by the complete blockage of the pores, hindering gas transport through the GDE, and eventual short-circuiting of the cell.

Despite the similar total currents, the partial current densities (j_{CO} and j_{H_2}) change notably with the GDE compression level (Fig. S2C). When the cathode spacing matches the thickness of the GDE, HER is preferred over CO_2R, resulting in $FE_{CO} \approx 25$ %. Increasing the compression level, j_{CO} increases, meanwhile j_{H_2} decreases, showing the suppression of the parasitic HER. At higher compression ratios (e.g., ~30 %), however, we experienced the rapid performance decay of the electrolyzer cell. This is most probably associated with the precipitate formation in the GDE, as experienced in earlier studies as well (see for example refs #21 and #23 in the manuscript). In this manuscript, therefore, all measurements were performed at ~15 % compression ratio, where the cell operation was found to be stable.

Linear sweep voltammetric measurements

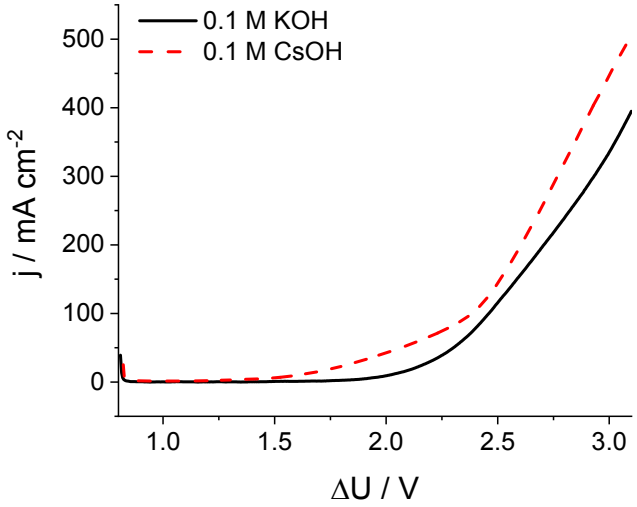

Fig. S3. LSV measurements applying different anolyte at T_{cell} = 60 °C. The CO_2 feed rate was 12.5 cm^3 min^{-1} cm^{-2} in both experiments.

Chronoamperometric measurements

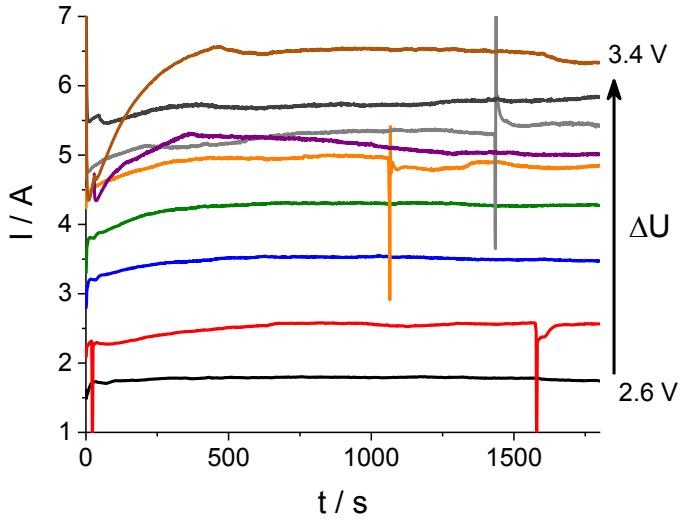

Fig. S4. Total cell current during chronoamperometric measurements at T_{cell} = 60 °C and different cell voltages. The CO_2 feed rate was 12.5 cm^3 min^{-1} cm^{-2}, and the anolyte was a 0.1 M CsOH solution for all the experiments.

Anode gas composition analysis and process stoichiometry

The mass balance of CO_2 electrolysis is presented in Fig. 4D in the m-s. Whether CO formation or H_2 evolution proceeds, the same amount of hydroxide ions (OH^-) form at the cathode (eq. 1-2). OH^- ions can further react with CO_2 to form HCO_3^- (eq. 3) or CO_3^{2-} (eq. 4). The negatively charged ions (OH^-, HCO_3^-, CO_3^{2-}) sustain the ion conduction, by passing through the AEM to the anode (note that the same amount of charge is transferred through the membrane as in the external electric circuit). We note that a minor fraction of the charge is carried by the Cs^+ (or K^+ etc.) ions, transporting in the opposite direction via unintended crossover. These could react with the formed HCO_3^-or CO_3^{2-} ions, leading to precipitate formation (eq. 5). The water management of the cell is complex: (i) the CO_2 feed is humidified, (ii) there is diffusion of water from the anode side to the cathode, (iii) ions cross the membrane in a hydrated form, (iv) water is consumed in reactions #2 and #6 (see Table S1), (v) the product stream also contains water.

Table S1. Chemical and electrochemical processes governing the mass balance of the CO_2 electrolysis process.

Electrochemical process at the cathode:	
$2CO_2 + 4e^- + 2H_2O \rightarrow 2CO + 4OH^-$	(1)
$4H_2O + 4e^- \rightarrow 2H_2 + 4OH^-$	(2)
Chemical processes at the cathode	
$2CO_2 + 4OH^- \rightarrow 2CO_3^{2-} + 2H_2O$	(3)
$4CO_2 + 4OH^- \rightarrow 4HCO_3^-$	(4)
$Cs^+ + HCO_3^- \rightarrow CsHCO_3$	(5)
Electrochemical process at the anode	
$2H_2O \rightarrow 4H^+ + O_2 + 4e^-$	(6)
$4OH^- \rightarrow 2H_2O + O_2 + 4e^-$	(7)
Chemical processes at the anode	
$4H^+ + 2CO_3^{2-} \rightarrow 2H_2O + 2CO_2$	(8)
$4H^+ + 4HCO_3^- \rightarrow 4H_2O + 4CO_2$	(9)
$4H^+ + 4OH^- \rightarrow 4H_2O$	(10)

Water or OH^- ions are oxidized at the anode to form O_2 (eq. 6,7). As shown in Table 1, the formed oxygen amount is one fourth that of the OH^- ions generated at the cathode. The anions formed at the cathode cross the membrane and react with the anodically formed H^+ ions (eq. 8-10). Pure O_2 gas would be detected at the anode, if only OH^- ions were responsible for the ion conduction through the AEM. However, transport of HCO_3^- and CO_3^{2-} ions through the membrane leads to CO_2 evolution, which is consequently present in the anode gas. Based on the stoichiometry of the electrochemical and chemical reactions depicted in the Table S1, the anode gas composition is 2:1 CO_2:O_2 if CO_3^{2-} is the exclusive charge carrier, while it is 4:1 in case of sole HCO_3^- conduction. The measured 66% CO_2 content of the anode gas (Fig. 4C in the m-s) suggests that CO_3^{2-} is the predominant charge carrier through the membrane.

Effect of the gas feed rate on the electrochemical performance

The CO_2 feed rate-dependence was also studied using the 32 μm thick PiperION membrane. j_{CO} increased first, then a slight decrease was seen upon further increase of the feed rate. The complexity of the water management of the cell might account for this non-trivial observation, and studies are in progress to uncover all mechanistic aspects.

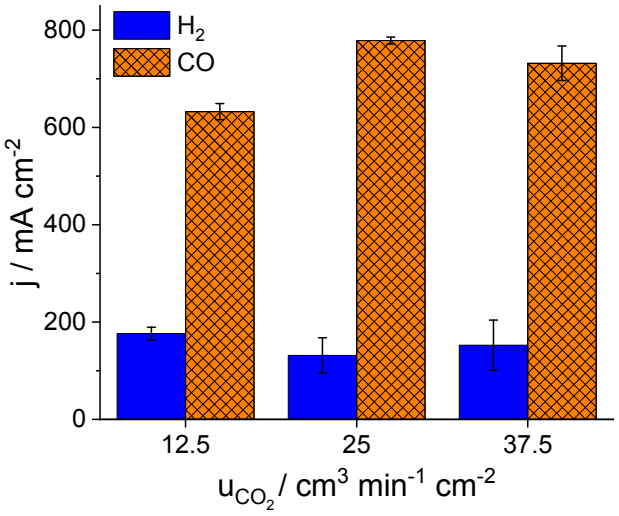

Fig. S5. Partial current densities for CO and H_2 formation during chronoamperometric measurements with a 32 μm thick PiperION membrane with 0.1 M CsOH anolyte at T_{cell} = 60 °C, ΔU = 3.4 V at different CO_2 feed rates.

Continuous electrolyzer operation with the PiperION membrane

The stability of the electrolysis process (including that of the 32 µm thick PiperION membrane) was assessed using 0.1 mol dm^{-3} CsOH anolyte and performing continuous electrolyzer for 8 hours at $\Delta U = 3.2$ V with 12.5 cm^3 min^{-1} cm^{-2} CO_2 feed rate. The CO production rate was 650 ± 50 mA cm^{-2}, and the FE remained between 70-80 % during the whole experiment.

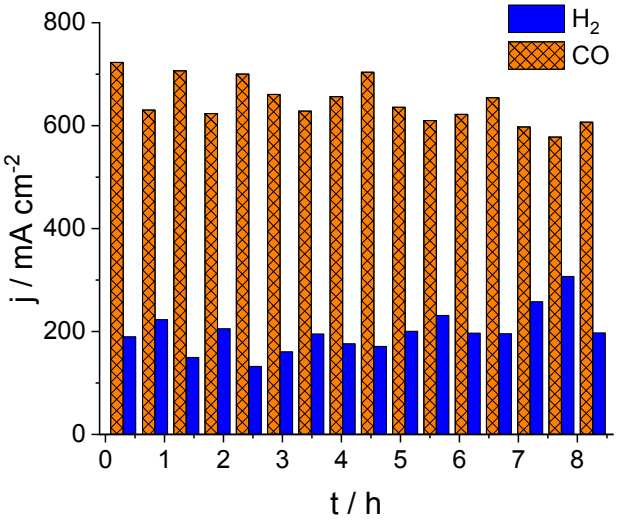

Fig. S6. Chronoamperometric measurement at $\Delta U = 3.2$ V cell voltage with u = 12.5 cm^3 min^{-1} cm^{-2} cathodic CO_2 feed rate and T = 60 °C 0.1 mol dm^{-3} CsOH anolyte concentration, using the 32 µm thick PiperION membrane.

Continuous operation with the PiperION membrane – the effect of CO_2 gas humidification

As mentioned in the manuscript, the gas humidification has a decisive effect on the cell operation. The same cell was assembled with identical components (32 µm PiperION membrane, 1 mg cm^{-2} Ag catalyst on Freudenberg H23C6 GDL cathode) and except for the gas humidification was operated under identical conditions (T = 60 °C, 0.01 M CsOH anolyte, ΔU = 3.2 V, 12.5 cm^3 min^{-1} cm^{-2} CO_2 feed). Clearly, j_{CO} increased by more than 50 % upon humidifying the gas stream, in T = 60 °C DI water (the temperature of the piping connecting the gas humidifier with the cell was maintained at 60 °C as well). Furthermore, the membrane was damaged (dried and burned locally) after 3 days of continuous operation in the non-humidified cell, leading to cell failure. In case of the cell operating with humidified CO_2 stream, no such membrane degradation (and cell performance fading) was revealed even after 150 h operation. Interestingly, the selectivity for CO production (FE_{CO}) was also higher with the humidified CO_2 gas feed.

We assume that the slow performance decay of the humidified CO_2 fed cell (Fig. S7) is related to the precipitate formation in the cathode GDE due to cation crossover from the anolyte, and its reaction with the electrogenerated hydroxide ions, - as experienced in earlier studies as well (see for example refs #21 and #23 in the manuscript). Using more concentrated anolyte solutions this effect occurs more rapidly, but even at this low concentration enough carbonate/bicarbonate precipitate forms in the GDE over a few days to block the gas path to the catalyst.

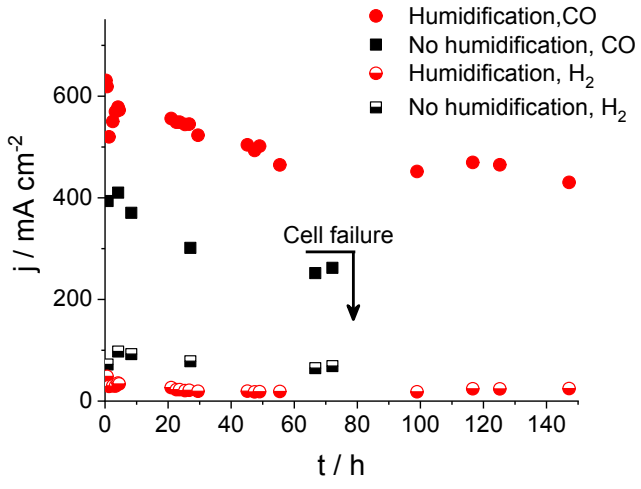

Fig. S7. Chronoamperometric measurements at T = 60 °C with 0.01 mol dm^{-3} CsOH anolyte and u = 12.5 cm^3 min^{-1} cm^{-2} cathodic CO_2 feed rate at ΔU = 3.2 V cell voltage.

Conductivity of the studied PiperION TP-85 membranes

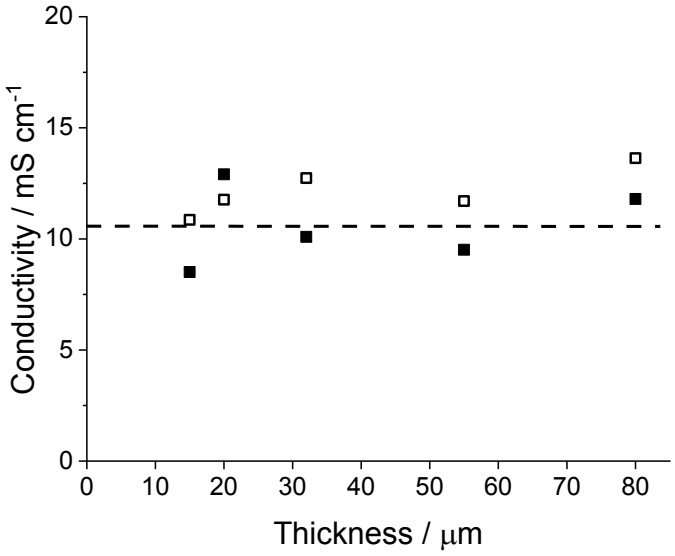

Fig. S8. Conductivity of the PiperION membranes with different thicknesses for HCO_3^- (filled) and CO_3^{2-} (open) ions, measured at T = 30 °C. The dashed line serves only to guide the eye.

Comparing the performance with PiperION and Sustainion® membranes of the same thickness

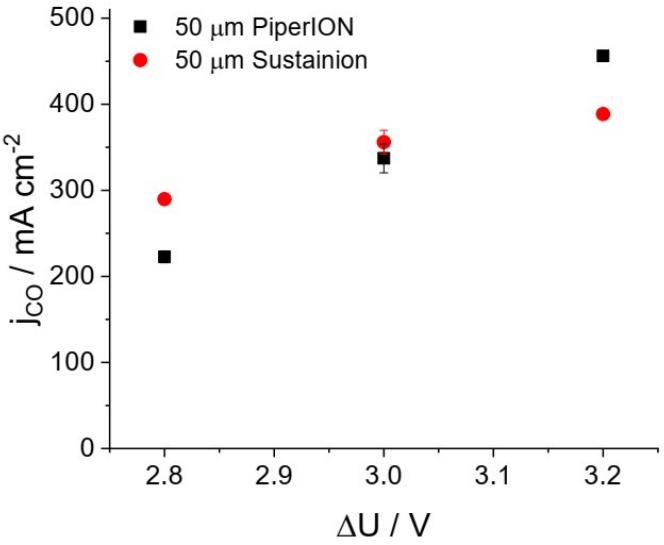

Fig. S9. Partial current densities for CO formation during chronoamperometric measurements with 0.1 M CsOH anolyte, at T_{cell} = 60 °C, 12.5 cm^3 min^{-1} cm^{-2} CO_2 feed rate and different cell voltages. The membranes were PTFE-reinforced Sustainion® (50 μm) and 50 μm thick PiperION. The ionomer was Sustainion® and PiperION respectively.

EIS spectra of cells assembled with PiperION membranes of different thickness

The high frequency intercept of the EIS spectra is directly related to the full cell resistance. As no other changes were made on the cell, its change is related to the membrane resistance. We found that the measured cell resistance scales with the membrane thickness: decreasing it from 80 to 15 μm in 4 steps the cell resistance changed from 0.92 to 0.66, 0.47, and 0.42 Ω cm^{-2}, respectively.

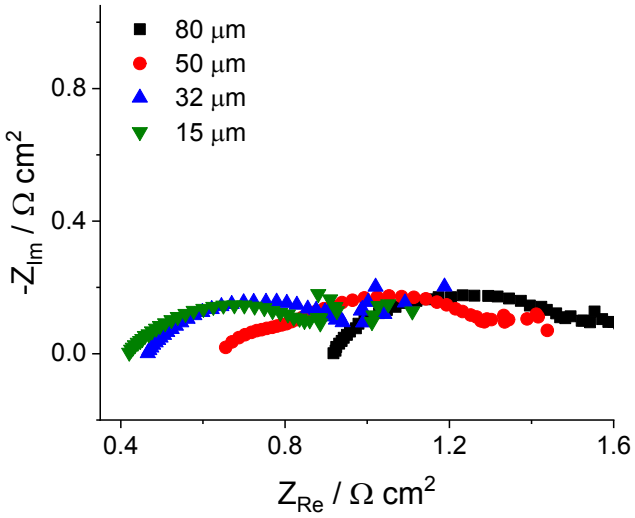

Fig. S10. EIS traces of electrolyzers assembled with PiperION membranes of different thickness, operated with T = 60 °C, 0.1 mol dm^{-3} CsOH anolyte, ΔU = 3.2 V, with u = 12.5 cm^3 min^{-1} cm^{-2} CO_2 feed rate.

Mechanical toughness test of PiperION and Sustainion® AEMs

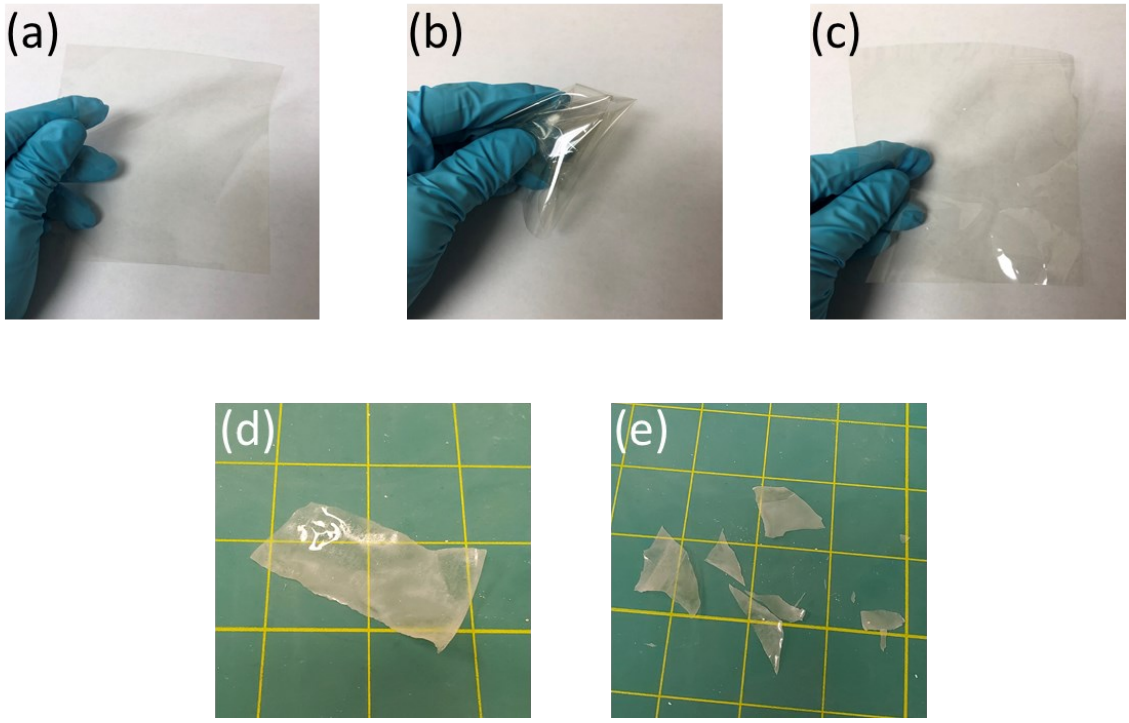

Fig. S11. Mechanical toughness test of PiperION AEM (50 μm) vs Sustainion® AEM (50 μm), both being in their bicarbonate form. (a) Fresh PiperION membrane. (b) Kneaded PiperION membrane. (c) Recovered PiperION membrane after (b). (d) Fresh Sustainion® AEM after 1M NaOH aq. treatment. (e) Dry Sustainion® AEM after being kneaded.

The mechanical properties of the two best performing AEMs are presented in Fig. S11 and S12. Due to the increased elongation of the PiperION membrane, it was necessary to rehydrate the membrane during the testing. This is the origin of the two perturbances shown in the plot (Fig S12.).

For the reinforced PiperION membrane, the plasticizer effect of water is less pronounced. It is seen that the stress at break is reduced from 52 MPa for the dry sample to 41 MPa for the wet sample. For the reinforced membrane, the yield point, seen as the inflection point of the line, shows no difference between the two conditions, demonstrating that the reinforcement is dominating the mechanical properties of the reinforced membranes. This is confirmed by the still high yield stress of the reinforced membrane when compared to the wet self-supporting membrane.

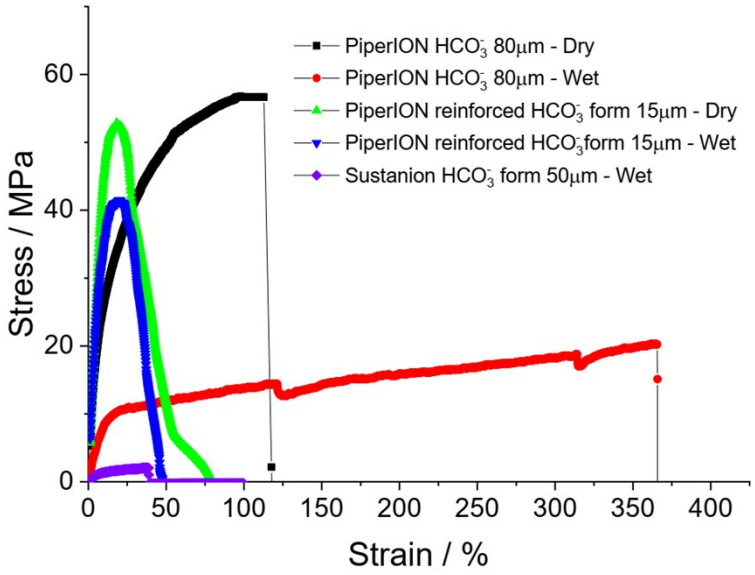

Fig. S12. Dynamic mechanical analysis data of PiperION and Sustainion® AEMs in their bicarbonate form. (Black) Stress–strain curve of fresh 80 μm PiperION at room temperature and ~50% RH. (Red) Fully hydrated 80 μm PiperION. (Green) Fresh 15 μm reinforced PiperION at room temperature and ~50% RH. (Blue) Fully hydrated 15 μm reinforced PiperION. (Purple) Fully hydrated 50 μm Sustainion® X37-50. All membranes were in their HCO_3^- form, and the tests were conducted with a strain rate of 10% min^{-1} at 25°C.

Formation of multi-electron reduction products from CO_2 using PiperION AEM

The use of the presented zero-gap electrolyzer cell and PiperION membrane is not limited to CO-generation. Employing a different cathode catalyst (for example Cu) in the process allows the formation of both ethylene and alcohols. While the optimization of the GDE structure and the process conditions points well-beyond the scope of this study, we have performed some exploratory measurements (Fig. S13). The formation of ethylene was confirmed at a partial current density ~100 mA cm^{-2} and with ~20% FE. In addition, the formation of ethanol and 1-propanol, with remarkable partial current density was also detected (together with trace amounts of formate and methanol). The exact quantification of liquid products, together with the process optimization is in progress.

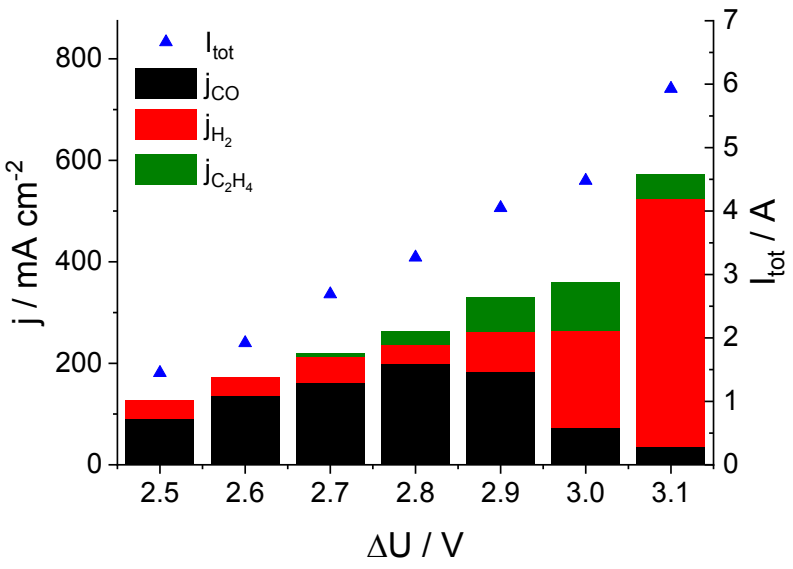

Fig. S13. Partial current densities at total current during chronoamperometric measurements with 0.1 M CsOH anolyte, at T_{cell} = 60 °C, 12.5 cm^3 min^{-1} cm^{-2} CO_2 feed rate and different cell voltages. The membrane was 32 µm thick PiperION, the cathode catalyst was spray-coated Cu nanoparticles (chemically deposited from $Cu(NO_3)_2$ according to ref [S1]) on Sigracet 39BC GDL. The catalyst layer further contained 15 wt% PTFE.

Reference

S1. J.-J. Lv, M. Jouny, W. Luc, W. Zhu, J.-J. Zhu and F. Jiao, *Adv. Mater.*, 2018, **30**, 1803111.